ELSEVIER

Journal of Power Sources 54 (1995) 411–415

JOURNAL OF POWER SOURCES

High reversible capacity carbon–lithium negative electrode in polymer electrolyte

R. Yazami, M. Deschamps

Laboratoire d'Ionique et d'Electrochimie du Solide de Grenoble (URA CNRS 1213), ENSEEG/Institut National Polytechnique de Grenoble, BP 75, 38402 Saint-Martin-d'Hères, France

Abstract

Cabonaceous materials from different types are used in polymer electrolyte-based lithium cells in order to evaluate their electrochemical performance during lithium storage in the application as the negative electrode in lithium-ion-type batteries. The formation of a passivating film during the first cathodic polarization may account for the low faradaic yield of the first cycle. It also plays an important role in the stabilization of the carbon/polymer electrolyte interface. Non-graphitized meso-carbon micro beads lead to a higher reversible capacity of 410 mAh/g than the graphitized one. It is suggested that lithium could be reversibly stored as a multilayer 'deposit' at the carbon surface. A model of epitaxial lithium electroplating is presented.

Keywords: Negative electrodes; Polymer electrolytes; Carbon; Lithium

1. Introduction

Pursuing our previous work on the electrochemical behaviour of the lithiated carbon negative electrode in polymer electrolyte [1] the performances of several carbonaceous materials from different origins expressed in terms of charge/discharge cycle efficiency, η_F, and reversible capacity, q_r, have been evaluated.

In natural or artificial graphite the theoretical capacity of 372 mAh/g is based on the assumption that lithium is totally stored in the intercalated state between the graphene layers to form the stage-1 compound LiC_6. The chemical intercalation of lithium in disordered carbons, using the so-called 'two bulb' method, yields lithium-deficient compounds Li_xC_6 where $x < 1$ consisting of mixtures of intercalation stages [2,3]. Therefore, it should be expected that reversible capacity of the electrode, q_r, with such carbon would be lower than the theoretical 372 mAh/g. Recently, several authors reported a q_r value higher than 372 mAh/g obtained in liquid electrolytes with non-graphitized carbons such as meso-carbon micro breads (MCMB) [4] or the pyrolysis product of polyphenylene [5]. Excess capacity was related to the contribution of the cavities present in MCMB to the lithium-reversible storage and to the possible occurrence of covalent bonds between lithium pairs which results in increasing the in-plane lithium density (Li_xC_6 where $x > 1$). The appearance of a reversible capacity associated not only to the intercalated lithium makes it difficult to predict the q_r values on the sole basis of the X-ray diffraction analysis which is more sensitive to the long-range order in the in- and out-plane organization rather than to the morphology of the carbon grains and surface defects [6].

In a recent work [7], we showed that under *C*/20 galvanostatic regime, natural graphite in fine powders could reversibly store up to 280 mAh/g in a poly(ethylene oxide) (PEO)-based electrolyte at 100 °C.

In this work we show that both the carbon/polymer electrolyte interfacial properties and some surface defects of the carbon may contribute to the faradaic yield during the first discharge/charge cycle and in the enhanced capacity in non-graphitized carbons. A new model involving the reversible epitaxial growth of lithium multilayers on the carbon planes is proposed to explain the observed high capacity.

2. Experimental

Different types of carbonaceous materials are used in this study:

(i) natural graphite (NG) from Madagascar was purified, ball milled and passed through a sieve of 200 mesh;

SSDI 0378-7753(94)02113-H

(ii) coal coke was provided by Carbone Lorraine (France) and consisted of a very fine powder (4 μm) with a narrow grain size dispersion;

(iii) MCMB in fine powders (6 μm) was provided by Osaka Gas (Japan) with two different heat treatments: 1000 °C (MCMB 6-10) and 2800 °C (MCMB 6-28) and

(iv) acetylene black (AB) for usual application as conducting additive was also evaluated in order to determine its relative contribution to the capacity of the composite electrode.

Composite electrodes consisting of a mixture of carbon, AB and PEO (used as binder) in weight ratio of 60/10/30 were prepared by spreading the mixture suspension in acetonitrile on a stainless-steel holder [8]. The Li/P(EO)$_8$–LiClO$_4$/carbon composite cells were operated at 100 °C and cycled under *C*/20 galvanostatic regime between 1.5 V and 5 mV.

In the NG-based cells, we have studied the electrode reaction mechanism by slow scan voltammetry (1 mV/min) between 0 and 0.3 V applied to a cell after a preliminary short circuit.

3. Results and discussion

3.1. Galvanostatic cycling

The first and second intercalation /de-intercalation cycles are given in Figs. 1 and 2. They show, that in a similar manner as in liquid electrolytes, the first cycle has a coulombic yield lower than the unity while that during the second cycle is close to the unity [9]. The reversible capacity after the first cycle remains constant for at least the next twenty cycles.

Table 1 gives the coulombic yield during the first and the second cycles, η_1 and η_2, together with the reversible capacity, q_r.

In ethylene carbonate (EC)-based liquid electrolytes, $\eta_1 < 1$ is attributed to the EC reduction at the surface of the carbon–lithium electrode [9]. In the PEO electrolyte, the initial wetting of the carbon electrode is rather poor compared with liquid electrolytes. This strongly affects the lower faradaic efficiency during the first cycle. In addition, it was observed that the lithium intercalation into graphite from a PEO-based electrolyte proceeds in two steps: (i) lithium plating on the carbon surface, and (ii) lithium intercalation between graphenes [10]. Moreover, Croce and Scrosati [11] showed that a passivation film is also formed at the metallic lithium/POE interface in a similar way as in the liquid electrolytes. Therefore, during the initial plating of lithium on the carbon surface, it is not excluded that PEO may react with the plated metal to form a new passivation film. This irreversible reaction should also contribute to the lower η_1 values. The strong interaction between plated lithium and the ether group may induce some polymer-chain dynamics resulting in an improved electrode wetting by the PEO (the chains tend to adhere on the carbon surface via O-Li bonds). This phenomenon tends to improve the cycling efficiency after the first cycle.

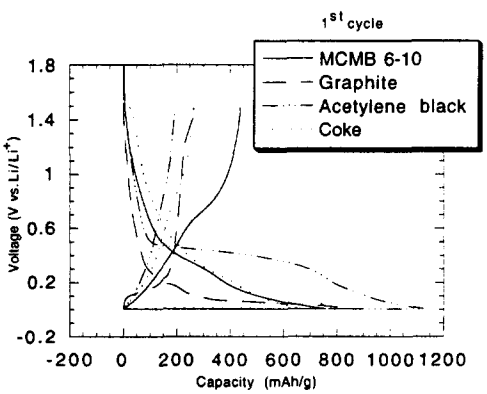

Fig. 1. First discharge/charge cycle of the Li/P(EO)$_8$–LiClO$_4$/carbon cells under *C*/20 galvanostatic regime.

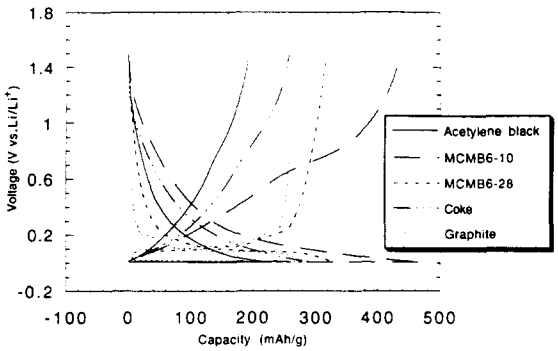

Fig. 2. Second discharge/charge cycle of the Li/P(EO)$_8$LiClO$_4$/carbon cells under *C*/20 galvanostatic regime.

Table 1
Performance data of various carbonaceous materials in PEO–LiClO$_4$-based cells as deduced from Figs. 1 and 2; η_1 and η_2 = faradaic yield of the first and second cycles, q_r = reversible capacity

Carbon	q_1 (mAh/g)	η_1 (%)	q_r (mAh/g)	η_2 (%)	x in Li$_x$C$_6$
Acetylene black	1117	17	190	96	0.52
Graphite	933	30	280	98	0.75
Coke	812	40	325	98	0.87
MCMB 6-28	1183	30	355	97	0.95
MCMB 6-10	1025	60	410	98	1.1

Additional lithium can be lost due to the formation of a residual lithium–carbon compound as generally observed in chemically intercalated carbons. In graphite, such residual compound may account for 10% of the lost lithium [2].

Table 1 reports data on the reversible capacity q_r obtained after the first intercalation/de-intercalation cycle and the corresponding relative amount of lithium x in reversibly exchanged Li$_x$C$_6$. Noteworthy is the

relatively high q_r reached with AB of 190 mAh/g while in liquid electrolyte this value did not exceed 90 mAh/g [12]. AB, in general, has the highest structure compared with other carbon blacks (oil furnace blacks, channel blacks or thermal blacks). This confers an increased electrical conductivity to the composite electrodes. In addition, the surface composition of the AB nodular particles should allow better compatibility with PEO than with liquid electrolytes due to their surface functions. This means that the wetting factor, which strongly affects the interfacial properties, plays the major role in the higher q_r values of AB. The higher crystalline organization of AB also should contribute to enhance q_r.

The interfacial properties of the lithiated NG/POE may also account for the low value of q_r of 280 mAh/g obtained with NG. NG is known for its low surface energy which allows its use as lubricant. This feature may hinder the formation of an adhesive POE-based film with a high coverage power.

Even though coal coke has a lower crystallinity than graphite, its obtained q_r value is higher (325 mAh/g). This result is even more evident when a comparison is made between two MCMBs before and after the graphitization treatment, MCMB 6-10 and MCMB 6-28, respectively. Graphitization leads to a decreased q_r from 410 mAh/g to 355 mAh/g in addition to better interfacial properties in MCMB 6-10 which gives a higher first cycle faradaic yield η_1 of 60% compared with 30% in MCMB 6-28.

The reason why q_r exceeds the theoretical value of 372 mAh/g for LiC_6 should be found in the different types of site occupied by the stored lithium. As a matter of fact, lithium can occupy either the available space between the carbon layers (intercalated lithium) or can be deposited as a multilayer on the carbon surface (multilayer lithium) or even interact with the carbon surface functions (oxygen, nitrogen, etc.).

Multilayer lithium is an intermediary state between the true intercalated lithium with a full charge transfer to the carbon hexagon (ionic-type bonding) and metallic lithium. In order to avoid the formation of lithium dendrites [13] which may lead to internal short circuit, multilayers of lithium of non purely metallic bonding-type should be favoured by a minute control of the electrode potential ($e \geq 0$ versus Li^+/Li). This can be achieved if a more or less complete charge transfer takes place between lithium and the carbon π orbital. In the LiC_6 network, lithium occupies the α-sites in the centre of the carbon hexagon as shown in Fig. 3, the first and closest to graphene lithium layer. If further lithium is deposited on the surface, the most thermodynamically stable site should be the epitaxial one on the β-site as shown in Fig. 4. Because the Li–Li distance should be kept lower than in covalent lithium (2.68 Å), the lithium of the β-sites will form a second

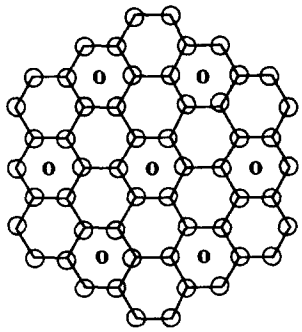

Fig. 3. In-plane hexal structure of LiC_6.

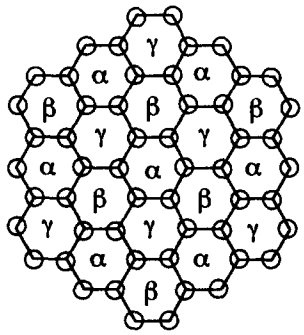

Fig. 4. Structure model of multilayered deposit lithium on the carbon *a*, *b* plane.

layer. The charge transfer to the graphene should be lower than in the α-layer because of lower orbital overlapping (increased C–Li distance) and of the necessary formation of a partial covalent bonding with this first α-layer to reduce the electrostatic repulsion. Similarly, a third layer can be formed with lithium on the available γ-site. The charge transfer to the carbon decreases from α- to β- and γ-layers. If further lithium is deposited, there must be a strong tendency to form pure alkali metal as a result of the total screening of the carbon layers. The formation of epitaxial multilayers on the graphene surface was reported during the low-temperature adsorption of molecules such as krypton with up to five layers [14], benzene [15] and ethylene [16].

The impurities present on the carbon surface can also favour the formation of intercalated multilayers of alkali metals as recently reported by Hérold et al. [17] in the case of potassium (double layer). These impurities tend to lower the electrostatic repulsion between the close-packed metal layers.

When the carbon electrode was subjected to decreasing lower potential values from 100 to 10 mV and −15 mV versus Li^+/Li during the lithium intercalation into coal coke, the reversible capacity was increased from 195 to 279 mAh/g and to 325 mAh/g, respectively. This is illustrated in Fig. 5 where the x values in Li_xC_6, exchanged at the end of the intercalation and de-intercalation sequences, are reported.

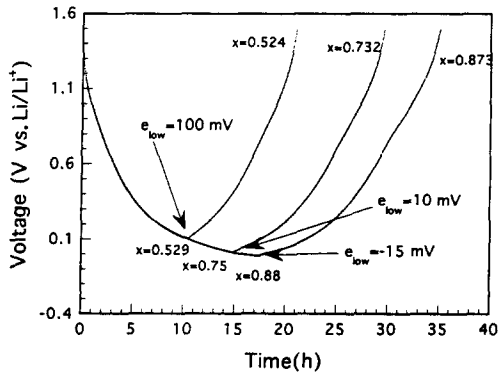

Fig. 5. Specific capacity vs. lower potential of the Li/P(EO)$_8$–LiClO$_4$/coal coke cell under *C*/20 galvanostatic regime.

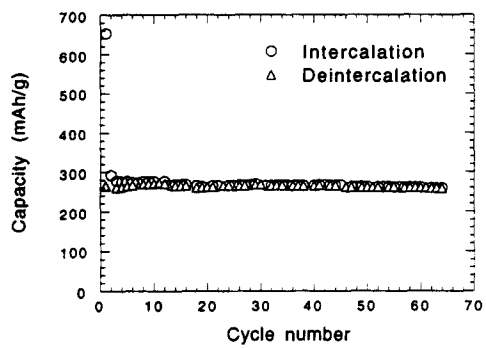

Fig. 6. Specific capacity vs. cycle number of the Li/P(EO)$_8$–LiClO$_4$/coal coke cell under *C*/20 galvanostatic regime.

Lower potential should favour the formation of lithium multilayers in addition to the intercalation. However, cycle life was much affected by the negative value under which lithium dendrites may be formed. The cell was not anymore operating after some cycles, at −15 mV as lowest potential, whereas more than 60 cycles could be reached at the potential limit of 10 mV, as shown in Fig. 6.

3.2. Cyclovoltammetry

The voltammogram given in Fig. 7 was obtained with NG-based electrode after an initial cell short circuit to full discharge. It shows, successively, oxidation (lithium de-intercalation) and reduction (lithium intercalation) peaks with differences in behaviour. The intercalation steps are more defined as shown by the separated peaks. These latter are attributed to the stage formation during the lithiation of NG. Assuming the stage-1 LiC_6 compound is obtained at the end of the most intense reduction peak at about 55 mV versus Li^+/Li, the other peaks at about 90, 135, 150 and 195 mV, respectively, could be ascribed to the stage-2, 3, 4 and 5 formation.

The differences in the shape of the reduction and oxidation peaks is the signature of differences of the electrode reaction mechanism. During intercalation, the

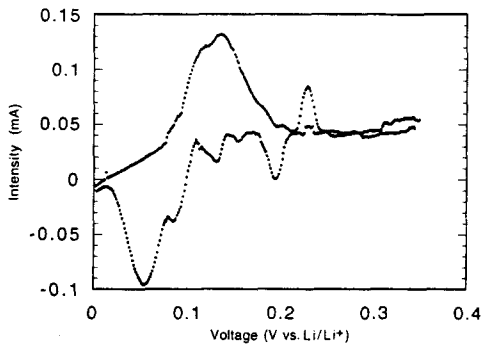

Fig. 7. Slow scan (1 mV/min) voltammogram of a Li/P(EO)$_8$–LiClO$_4$/natural graphite cell after a short circuit applied for 1 day at 100 °C.

graphenes must be separated from each other to allow the accommodation of the lithium ion. The energy needed to separate these layers generates a potential delay between each step, and therefore, the reduction peaks are well separated. During the de-intercalation of lithium, a more collective behaviour is observed since the driving force to extrude lithium from the layers is higher. This results in the appearance of a broader oxidation peak showing only shoulders rather than defined peaks.

The last isolated oxidation peak at 215 mV should be attributed to the formation of graphite from high-stage graphite-intercalation compounds.

It is worth noticing that in the 0–220 mV range, almost all the lithium has been intercalated and de-intercalated into/from graphite indicating that the lithium–graphite electrode keeps a very low working potential in agreement with previously reported results [18]. This may be related to the lower concentration of lattice defects in natural graphite which allows a more homogeneous distribution of the transferred charge from lithium to the conducting π-band and leads to a lower potential compared with NG carbons.

References

[1] R. Yazami and Ph. Touzain, *J. Power Sources, 9* (1983) 365.
[2] D. Guérard, *Ph.D. Thesis*, University of Nancy, France, 1974.
[3] R. Yazami and D. Guérard, *J. Power Sources, 43,44* (1993) 39.
[4] A. Mabuchi, K. Tokomitsu, H. Fujimoto and T. Kasuh, in *Ext. Abstr., 7th Int. Meet. on Lithium Batteries, Boston, MA, USA, 15–20 May, 1994*, p. 212.
[5] K. Sato, M. Noguchi, A. Demachi, N. Oki and M. Endo, *Science, 264* (1994) 556.
[6] J.R. Dahn, A.K. Sleigh, H. Shi, B.M. Way, W.J. Weydanz, J.N. Reimers, Q. Zhong and U. von Sacken, in G. Pistoia (ed.), *Lithium Batteries, New Materials, Developments and Perspectives*, Elsevier, 1994, and refs. therein.
[7] R. Yazami, K. Zaghib and M. Deschamps, *J. Power Sources, 52* (1994) 55.
[8] R. Yazami, in A.P. Legrand and S. Flandrois (eds.), *Chemical Physics of Intercalation*, Nato ASI Ser., Ser. B: Physics, Vol. 172, 1987, pp. 457.

[9] R. Fong, U. Von Sacken and J.R. Dahn, *J. Electrochem. Soc., 137* (1990) 2009.
[10] R. Yazami and Ph. Touzain, *J. Power Sources, 9* (1983) 365.
[11] F. Croce and B. Scrosati, *J. Power Sources, 43/44* (1993) 9.
[12] O. Chusid, Y. Ein Ely, D. Aubach, M. Babai and Y. Carmelli, *J. Power Sources, 43/44* (1993) 47.
[13] R. Selim and P. Bro, *J. Electrochem. Soc., 121* (1974) 1467.
[14] J. Menancourt, A. Thomy and X. Duval, *J. Phys. (France), 38-C4* (1977) 194.
[15] Y. Khatir, M. Coulon et L. Bonnetain, *J. Chem. Phys., 75* (1978) 789.
[16] J.C. Delachaume, M. Coulon and L. Bonnetain, *Surf. Sci., 133* (1983) 365.
[17] C. Hérold, M. El Gadi, J.F. Marêché and Ph. Lagrange, *Mol. Cryst. Liq. Cryst., 244* (1994) 41.
[18] R. Yazami, A. Cherigui, V. Nalimova and D. Guérard, *Proc. Symp. Lithium Batteries, The Electrochemical Society 182nd Fall Meet., Toronto, Canada, 11–16 Oct. 1992,* Proc. Vol. 93-24, The Electrochemical Society, Pennington, NJ, USA, 1993, p. 1.